ELSEVIER

Sensors and Actuators A 93 (2001) 258–265

SENSORS AND ACTUATORS A PHYSICAL

www.elsevier.com/locate/sna

The diagnostic micromachined beams on (1 1 1) substrate

Hsin-Hwa Hu[a], Hung-Yi Lin[a], Weileun Fang[a,*], Bruce C.S. Chou[b]

[a]*Power Mechanical Engineering Department, National Tsing Hua University, Hsinchu 30043, Taiwan, ROC*
[b]*Precision Instrument Development Center, Hsinchu, Taiwan, ROC*

Received 20 October 2000; accepted 16 April 2001

Abstract

The undercut process of the micromachined structures on a (1 1 1) oriented silicon wafer is studied in this paper. As observed in the experiment, the undercut of a cantilever on (1 1 1) wafer is along the width of the beam. According to the undercut mechanism, the advantages of fabricating a cantilever on (1 1 1) wafer are three-fold: (1) significantly reduce the etching time and obtain an ideal clamped boundary in the mean time; (2) the thickness as well as the moment of inertia of the cantilever is closer to the ideal case; (3) the flexural rigidity of the cantilever is constant along the beam axis. Consequently, the micromachined cantilever on a (1 1 1) wafer is more appropriate in various applications. For instance, it is more appropriate to fabricate the diagnostic microstructures on the (1 1 1) wafer than on the (1 0 0) wafer in determining the thin film residual stress.

Keywords: Substrate; Micro diagnostic structure; Thin film residual stress

1. Introduction

The wet anisotropic etching of a single crystal silicon substrate is an important fabrication technique in bulk micromachining. The primary feature of this process is that etching rate of the substrate depends upon its crystallographic orientation. For instance, the etching rate of the {1 1 1} planes of a single crystal Si wafer is extremely slow for various etching solutions [1]. Thus, the {1 1 1} planes are usually exploited to stop the etching in a specific direction on the Si wafer during anisotropic etch. On the other hand, the {1 0 0} planes have higher etching rate in anisotropic etchant [1,2]. The wet anisotropic etching technique is mainly applied to the (1 0 0) and (1 1 0) oriented Si wafers so far [3].

A rectangular pit illustrated in Fig. 1a is bounded by the {1 1 1} crystallographic planes on the (1 0 0) wafer for any arbitrary opening of the mask pattern [4]. As shown in Fig. 1a, the intersection lines of these {1 1 1} crystallographic planes and the wafer surface form a rectangle. To fabricate highly symmetric micromachined structures is thus possible. In addition, to design patterns of micromachined structure is easy since the undercutting mechanism of the (1 0 0) oriented Si wafer has been through studied [5–7]. The (1 0 0) oriented Si wafer becomes the most common substrate used in the fabrication of microstructures.

The (1 1 1) oriented Si wafer is rarely used in micromachining, since the {1 1 1} crystallographic planes prevent the Si wafer from being bulk etched. A hexagonal pit illustrated in Fig. 1b is bounded by the {1 1 1} planes on the (1 1 1) oriented Si wafer for openings with any arbitrary shape [8]. However, this process requires very long etching time. The technique to conduct undercutting process for wet anisotropic etching on (1 1 1) oriented Si wafer has been proposed. The idea of this approach is to etch the substrate by reactive ion etching (RIE) [8,9] or isotropic wet etching [10] before anisotropic wet etching. The crystal planes, which are not {1 1 1} oriented, will be exposed and anisotropic chemical etching occurs in this manner. Thus, the micromachined structures, such as cantilevers, bridges, and suspensions are available on (1 1 1) oriented Si wafer after anisotropic bulk etching.

Microcantilever is one of the major diagnostic structures for measuring mechanical properties of thin film, such as residual stress [11], Young's modules [12] and thermal expansion coefficient [13]. The way to predict thin film residual stress by microbridge is also mature [14,15]. Boundary conditions and beam geometry (especially thickness) of these diagnostic structures are key factors of measurement accuracy. This research investigates the undercut mechanism of the (1 1 1) oriented Si wafer. The superiority of (1 1 1) wafer over (1 0 0) wafer as the substrate of

* Corresponding author. Tel.: +886-3-574-2923; fax: +886-3-572-2840.
E-mail address: fang@pme.nthu.edu.tw (W. Fang).

0924-4247/01/$ – see front matter
PII: S0924-4247(01)00652-5

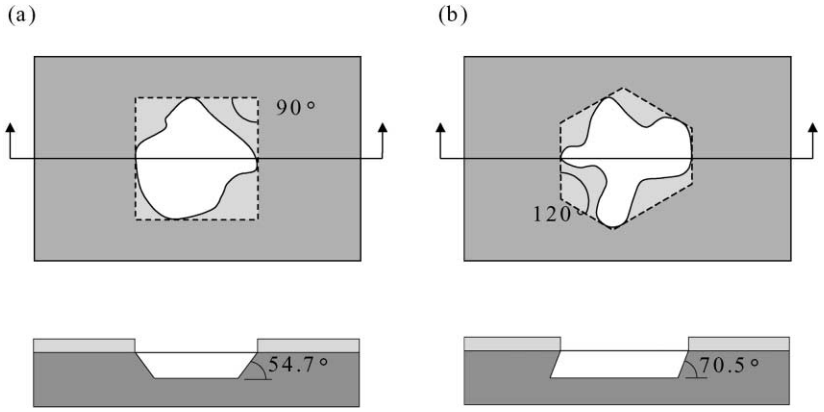

Fig. 1. Top view and side view of {1 1 1} planes in both (a) (1 0 0); and (b) (1 1 1) oriented silicon wafers.

thin film diagnostic structures was hence presented. At first, undercutting time was substantially reduced. Then, the micro beam is prismatic (cross-section is uniform along beam length) so stiffness is also constant. In addition, a better-clamped boundary of micro bridge is accessible.

2. Experiment and results

Fig. 2 schematically shows the processes used in this study to fabricate micromachined beams on a (1 1 1) oriented Si wafer. A silicon dioxide thin film was thermally grown on a p-type single crystal silicon substrate with (1 1 1) orientation. The transparent SiO_2 film was used to fabricate micromachined structures for observing the undercut processes during etching. After the SiO_2 film was patterned by photolithography and buffered HF as shown in Fig. 2b, the silicon substrate was etched by RIE as shown in Fig. 2c. Therefore, the silicon substrate can be removed anisotropically by 15% KOH solution at 75°C. The illustrations in Fig. 2d and e, respectively, show the cross-sections BB′ and AA′ indicated in Fig. 2a after anisotropic etching.

The photograph in Fig. 3a shows a SiO_2 microbridge on the (1 1 1) wafer. Fig. 3a demonstrates that the opening of arbitrary shape on a mask would form a hexagonal cavity after sufficient etching time. The opening would be almost perfectly inscribed in this hexagonal cavity after anisotropic etching [8]. The side walls being the slow-etching {1 1 1} crystal planes formed the hexagonal cavity. After the substrate was etched by RIE, it took 12 min to fully undercut a 16 μm wide, 120 μm long microbridge. In this case, one pair of the (1 1 1) planes is aligned perpendicular to the bridge length to form the ideal clamped boundary after anisotropic etching. As indicated in Fig. 2e, one of the boundaries would be slightly undercut, and its magnitude is about 35% of the RIE depth. This will lead to asymmetry boundary to the microbridge. But, the depth of RIE is small when fabricating a diagnostic structure, this undercut is not evident. For instance, the amount of boundary undercut in this research is only 1 μm. However, precise etching time is needed to fabricate bridges with ideal clamped boundary on (1 0 0) substrate-otherwise concave corners beneath would change the mechanical behaviour of micro bridges as illustrated in Fig. 3b and c. The critical buckling load and resonance frequency might deviate evidently.

In order to determine the undercut processes on the (1 1 1) wafer, microcantilevers with various length and width were fabricated. The photographs in Fig. 4 display the undercut processes of three 16 μm wide microcantilevers with length from 96 to 120 μm. It is obtained that the undercut is along

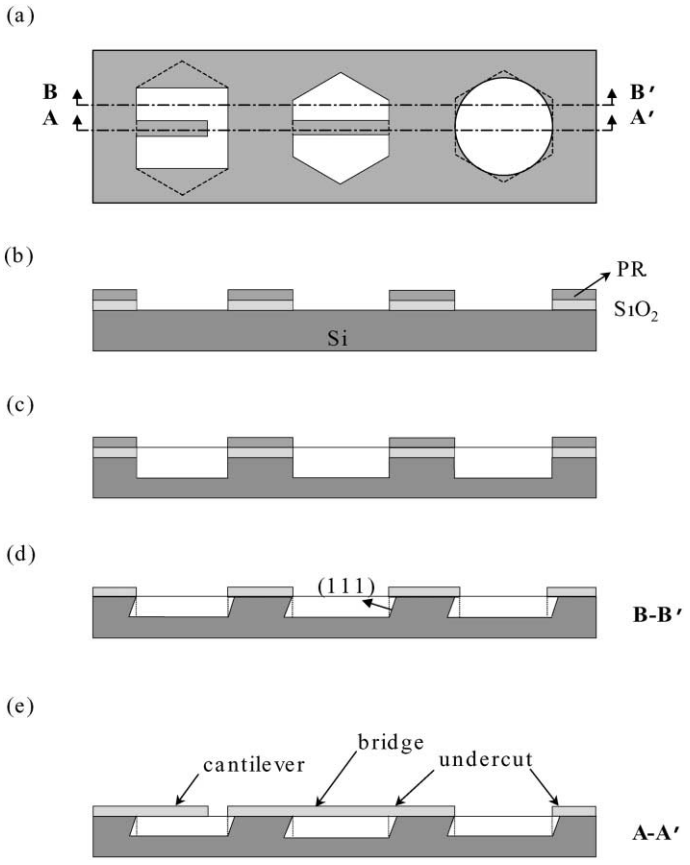

Fig. 2. Fabrication processes of structures on (1 1 1) oriented Si wafer.

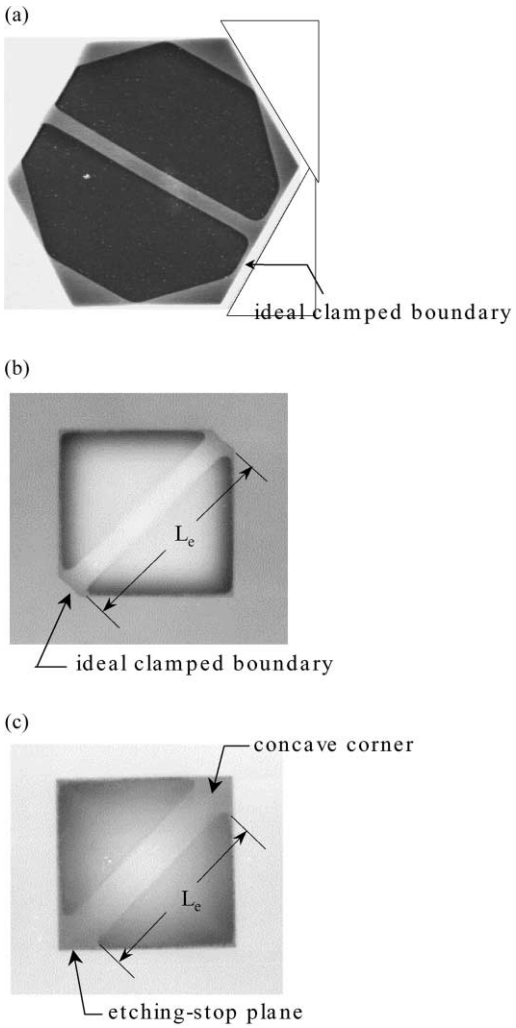

Fig. 3. Microbridges on the cavity of (a) (1 1 1) substrate with ideal clamped boundaries; (b) (1 0 0) substrate with ideal clamped boundary; (c) (1 0 0) substrate with concave corner.

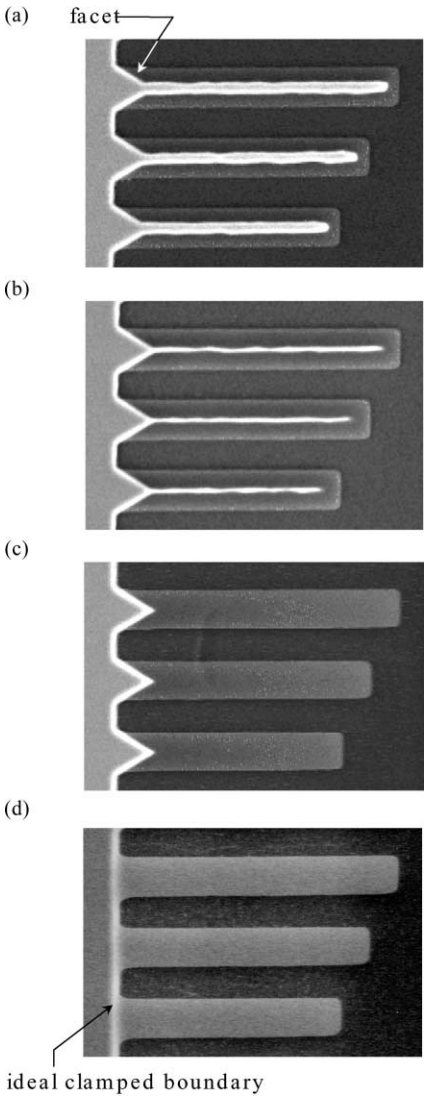

Fig. 4. OM photographs of microcantilever undercut process on (1 1 1) wafer when etch time is (a) 4; (b) 5; and (c) 12 min.

the width of the beam. There were two facet planes appearing at the end of the beam during etching is also observed, as indicated in Fig. 4a. The circumscribed-hexagon {1 1 1} planes of the opening area resulted in the facet planes. After etching for 6 min, the two facet planes met and formed a triangular region with the boundary of the beam, as shown in Fig. 4c. In Fig. 4d, the triangular region was etched away due to the convex corner effect until the (1 1 1) crystallographic plane at the end of the beam was reached. The undercut process from Fig. 4c to d was ca. 6 min. Fig. 4 reveal that width but not length of the beams determines the etching time since the undercut is mainly along the width of the beams. According to the experiment, to fully undercut all of the 16 μm wide microcantilevers with arbitrary beam length on a (1 1 1) wafer takes about 12 min. In short, this process significantly reduces the etching time needed to fully undercut a longer microcantilever with ideal clamped boundary on (1 1 1) wafer.

3. Discussion

3.1. Undercut mechanism

The undercut phenomenon is a very important characteristic for anisotropic etching. This phenomenon has been used widely to fabricate micromechanical structures [7,16]. The cantilever illustrated in Fig. 5a is located at a rectangular opening on a (1 0 0) oriented Si wafer. To allow the boundary of the cantilever perfectly clamped to the substrate, the edges of the opening and that of the cantilever are all aligned to the ⟨1 1 0⟩ directions. The (1 1 1) crystallographic planes, therefore, stop the undercut from the edge of the cantilever. In such a circumstance, the undercut of the cantilever, as indicated by the dash lines in Fig. 5a, results from the convex corner effect along the length of the beam [1]. Although this approach can fabricate a cantilever, it needs long etching time. In addition, the cantilever would crack due to the stress

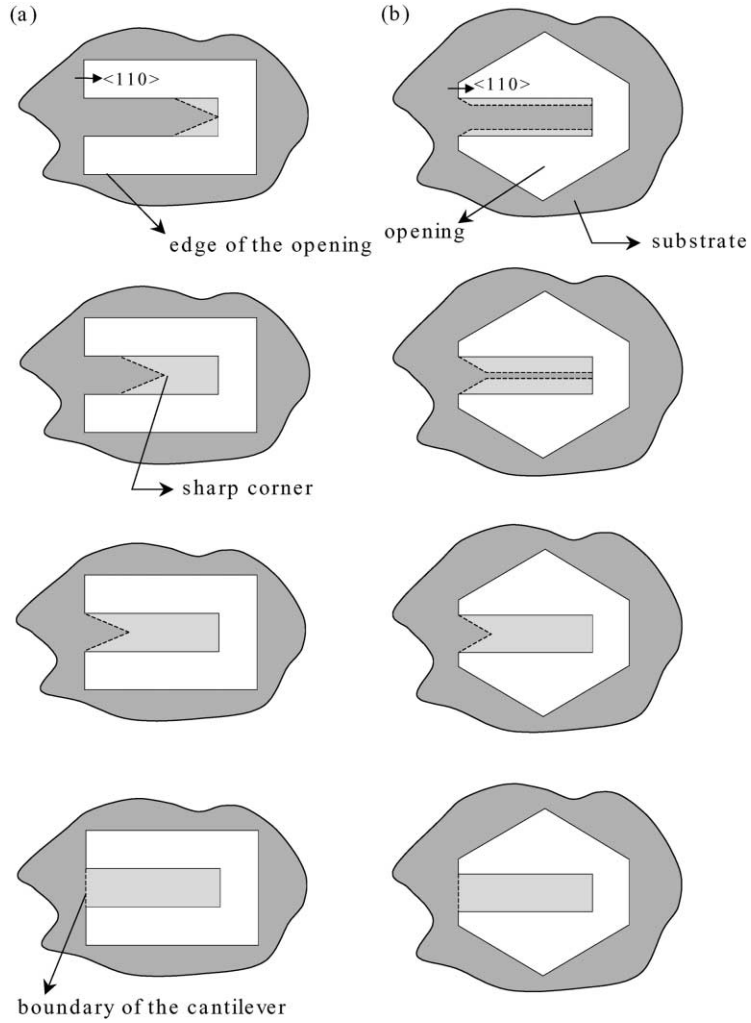

Fig. 5. Undercut process of a microcantilever on the (a) (1 1 1); and (b) (1 0 0) oriented wafer.

concentration effect at the tip of the sharp corner shown in Fig. 5a [17]. Tilting the mask pattern can significantly increase the undercut rate. However, the cantilever would be connected to a deformable suspension instead of the Si substrate.

According to the experiment, the undercut processes of the cantilever on a (1 1 1) oriented Si wafer are displayed in Fig. 5b. The cantilever illustrated in Fig. 5b is located at a hexagonal opening on a (1 1 1) oriented Si wafer. The boundary of the cantilever is perfectly clamped to the substrate since the edges of the cantilever are aligned to the $\langle 1\ 1\ 0 \rangle$ directions. The undercut mechanism gives the (1 1 1) Si wafer several advantages over the (1 0 0) Si wafer in fabricating bulk micromachined beams. As indicated by the dash lines in Fig. 5b, the undercut of the cantilever is along its width. This undercut process prevents the cantilever from cracking due to the stress concentration effect of the sharp corner. The etching time t_1 needed to fabricate a cantilever on a (1 1 1) Si wafer is independent of the beam length. The measured results shown in Fig. 6 indicate that

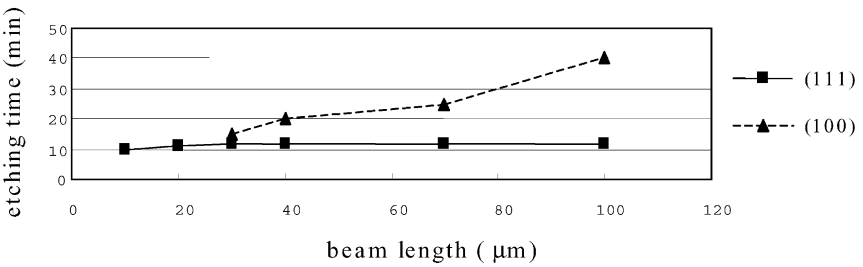

Fig. 6. The relation between beam length and etching time for cantilevers on both (1 0 0) and (1 1 1) substrates.

the etching time t_1 for 16 μm wide and 30–120 μm long cantilevers are around 10–12 min. On the other hand, the etching time t_2 needed to fabricate a cantilever on a (1 0 0) Si wafer is increased with the beam length. In Fig. 6, the etching time t_2 for 16 μm wide and 50–120 μm long cantilevers are increased from 15 to 40 min. As compared with the (1 0 0) Si wafer, the etching time t_1 required to fabricate a cantilever on a (1 1 1) Si wafer is significantly reduced for a longer cantilever.

3.2. Geometry and deflection of the beam

In the experiment, the etching rate r_e of the thermally grown SiO_2 film under the KOH solution is about 105 nm/h. Thus, anisotropic bulk etching would change the cross-section as well as the thickness of the SiO_2 beam. As indicated by the dashed lines in Fig. 7, the ideal cross-section of the cantilever has a width w_0 and a thickness h_0 by assuming that the KOH etchant has infinite selectivity for the silicon substrate over the SiO_2 film. Assume that the silicon substrate and the SiO_2 film are etched at a uniform rate. After the removing of the SiO_2 film is considered, the thickness h_1 and the width w_1 of the cantilever on (1 1 1) wafer become $h_1 \approx h_0 - 2d_1$ and $w_1 = w_0 - 2d_1$, respectively. As shown in Fig. 7b, the cross-section of the beam on (1 1 1) wafer becomes a pentagon instead of a rectangle. However, the cantilever in Fig. 7b remains a prismatic beam. Although the cross-section of the cantilever on a (1 0 0) oriented Si wafer remains a rectangle; its thickness is expressed by

$$h_2 = h_0 - d_2\left(1 + \frac{x}{L}\right) \tag{1}$$

and varies linearly with the longitudinal location x of the beam, as illustrated in Fig. 7a. The thickness d_1 and d_2 vary linearly with the etching time t_i, and can be expressed as

$$d_i = r_e t_i \quad (i = 1, 2) \tag{2}$$

where r_e and t_i are determined from the experiment, and the subscript 1 and 2 indicate the (1 1 1) and (1 0 0) wafer, respectively.

This work also studied the differences of the mechanical properties between the cantilevers on (1 0 0) wafer and those on (1 1 1) wafer. The dimension of a typical test cantilever is 120 μm long, 16 μm wide and 0.6 μm thick. The ideal moment of inertia I_0 for this test cantilever is 0.288 μm^4. Since the etching time t_1 measured from the experiment is 12 min, it is calculated from Eq. (2) that $d_1 = 20$ nm. After considering the etching of the SiO_2 film, the moment of inertia I_1 for the test cantilever on (1 1 1) wafer is reduced from 0.288 to 0.246 μm^4. Thus, the decreasing of the flexural rigidity for the test cantilever on (1 1 1) wafer is ca. 15%. Since t_2 is 40 min for the test cantilever on (1 0 0) Si wafer, the d_2 obtained from Eq. (2) is 70 nm. Based on Eq. (1), the variation of the thickness between the tip and the end of the tapered cantilever on (1 0 0) wafer is 13%, as shown in Fig. 7a. The moment of inertia I_2 of the tapered cantilever varies from 0.198 to 0.131 μm^4 along the beam axis. As compared with the ideal cross-section, the flexural rigidity of the test cantilever on (1 0 0) wafer decreases 31% at $x = 0$ and decreases 56% at $x = L$.

The bending of a micromachined cantilever has been used to measure the residual stress of a thin film material [11]. In the existing approaches, a bending moment resulted from the residual stress bent the micromachined cantilever. The cantilever is regarded as a prismatic beam with a uniform flexural rigidity along the beam length. Consequently, the bending moment bent the micromachined cantilever with a

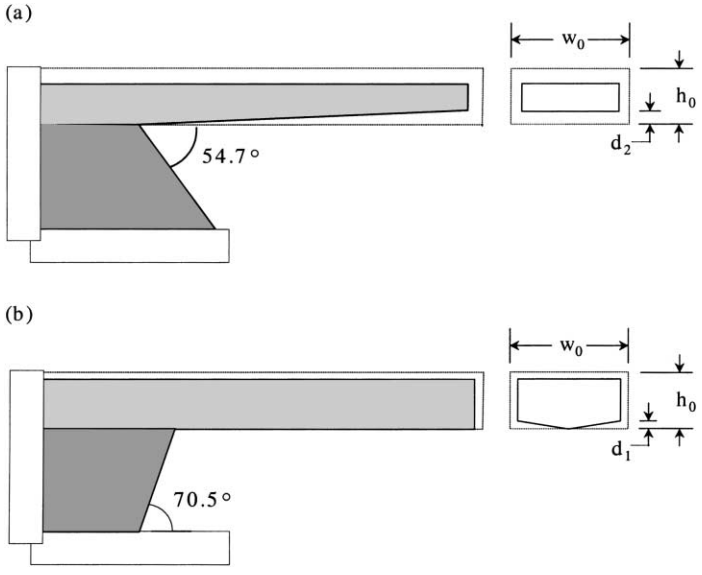

Fig. 7. Thickness variation of thin film on (a) (1 1 1); and (b) (1 0 0) oriented wafer after anisotropic etch of KOH.

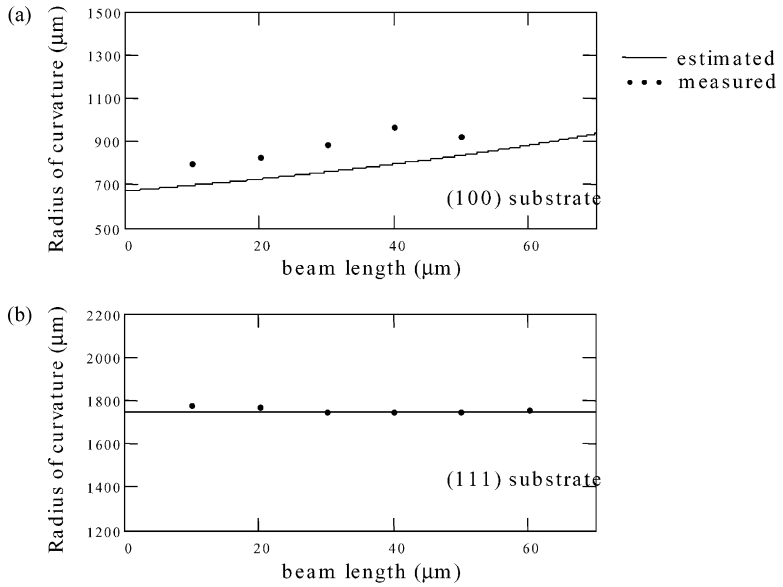

Fig. 8. Radius of curvature for micro cantilever beams on (a) (1 1 1); and (b) (1 0 0) oriented substrates.

constant radius of curvature R. The residual stress of a thin film can be determined if the radius of curvature R of the micromachined cantilever is measured. According to the present study, the thickness as well as the flexural rigidity of the cantilever on (1 0 0) wafer is not uniformly distributed along its length. The radius of curvature of the cantilever on (1 0 0) wafer bent by the thin film residual stress is no longer constant along the beam length. Fig. 8 shows the variation of the radius of curvature of a 60 μm long cantilevers along the beam axis. The dots in Fig. 8 indicate the average radius of curvature of the cantilever measured from the region between the boundary and the length shown in x-axis of the beam. As shown in Fig. 8a, the radius of curvature of the cantilever on (1 0 0) wafer measured within the range of 0–60 μm is $R = 900$ μm, and measured within the range of 0–10 μm is $R = 750$ μm. The variation of R with the beam length is 16.7% for a 60 μm long beam. The variation of R would increase for a longer beam. Thus, the approach presented in [11] has to be modified to improve the accuracy of the results. On the contrary, the radius of curvature of the cantilever on (1 1 1) wafer remains constant along the beam axis, as shown in Fig. 8b. In this regard, the cantilever on (1 1 1) wafer is a better test key to determine thin film residual stress.

The bilayer cantilever technique for determining the residual stress of very thin films had been reported in [18]. A bilayer beam is formed after depositing a very thin film onto a diagnostic micromachined cantilever. The radius of curvature of the cantilever would be changed from R (single layer cantilever) to R_1 (bilayer cantilever) due to the residual stress of the deposited film. The residual stresses of the deposited film will be determined after R and R_1 is measured. The thickness of the diagnostic micromachined

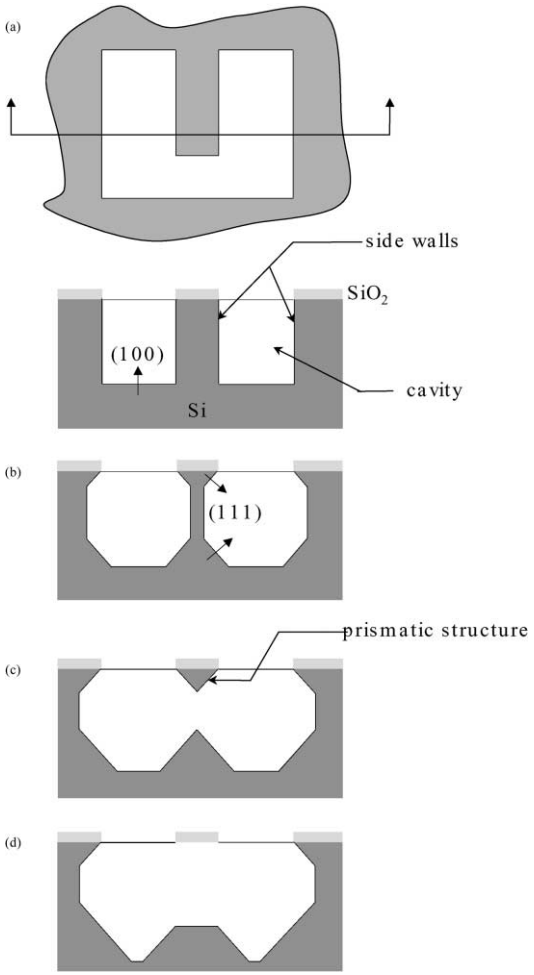

Fig. 9. Anisotropic etching prediction of cantilevers on (1 0 0) substrate when RIE depth is greater than $w_0 \tan 54.7^\circ$.

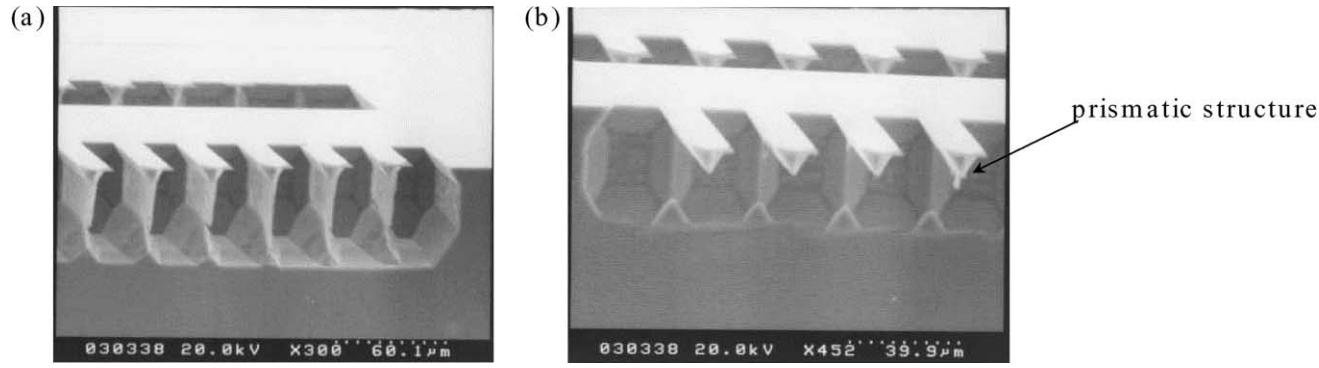

Fig. 10. SEM photos of undercut process for cantilevers on (1 0 0) substrate after Si RIE.

cantilever should be uniform to ensure the radius of curvature R_1 is a constant along the beam length. Otherwise the variation of R_1 would be significant. For instance, the variation of R_1 for the 100 μm long bilayer cantilever on the (1 0 0) substrate is 10–19%. Furthermore, the variation of R_1 will increase when the thickness of the deposited film decreases. This effect contributes a significant error in determining the properties of very thin film.

3.3. (1 0 0) cantilever beam with an additional Si RIE

The micromachining processes illustrated in Fig. 2 were also exploited to fabricate beams on (1 0 0) substrate. As shown in Fig. 9a and b, the anisotropic etching is initiated from the side walls of the cavities generated by RIE. It is obtained from Fig. 9b that the (1 1 1) crystal planes of the silicon substrate remain the slowest etching planes. As shown in Fig. 9c, these (1 1 1) crystal planes will form a prismatic structure with a triangular cross-section under the beam during etching. Since this prismatic structure contains a convex corner, the silicon material under the beam can be removed completely. Fig. 9d illustrates a beam fabricated through these processes. The experiment was conducted in this study to demonstrate the processes shown in Fig. 9. The SEM photos in Fig. 10 show the undercut of micromachined cantilevers by KOH right after the substrate etched by DRIE for 50 μm. The width of the cantilevers in Fig. 10a and b are 18 and 16 μm, respectively. The beam with smaller width w would be undercut faster than that with larger w in this experiment. Finally, it took 15 min to fully undercut the 18 μm wide cantilever.

Although micromachined beams can also be fabricated on the (1 0 0) substrate through the processes in Fig. 2, there are several disadvantages. The etching time for the (1 0 0) substrate is longer than that for the (1 1 1) substrate since an additional under etching process from Fig. 9c to d is required. In addition, the {1 1 1} crystal planes on the (1 0 0) substrate could stop the undercut process shown in Fig. 9 if the cavity generated by RIE is not deep enough. It is very difficult to fully undercut the silicon substrate in this case, since the walls of the pyramid pit stop the etching [5]. In short, if the depth etched by the RIE is smaller than $w_0 \tan 54.7^\circ$, the micromachined beams cannot be fabricated.

4. Conclusion

The variety of micromachined devices is rapidly increased with the growing of MEMS applications. In order to improve the performances of the microstructures, the (1 1 1) oriented silicon wafer is a better choice in compared with the (1 0 0) and the (1 1 0) wafer. This paper brings up some aspects of using (1 1 1) wafer as a substrate in bulk micromachining and tends to expand the variety of microstructures. According to the undercut mechanism, the advantages of fabricating a cantilever on (1 1 1) wafer are three-fold: (1) the etching time is significantly reduced; (2) the thickness as well as the moment of inertia of the cantilever is closer to the ideal case; (3) the flexural rigidity of the cantilever is a constant along the beam axis. The micromachined cantilever on a (1 1 1) wafer is more appropriate in various applications. For instance, the diagnostic structure can be used to determine the thin film residual stress.

Acknowledgements

This material is based (in part) upon work supported by the National Science Council (Taiwan) under Grant NSC 88-2218-E007-004. The author would like to express his appreciation to the NSC Central Regional MEMS Research Center (Taiwan), Electrical Engineering Department of National Tsing Hua University (Taiwan), Semiconductor Center of National Chiao Tung University (Taiwan), and National Nano Device Laboratories (Taiwan) in providing fabrication facilities.

References

[1] H. Seidel, L. Csepregi, A. Heuberger, H. Baumgartel, Anisotropic etching of crystalline silicon in alkaline solutions. Part 1. Orientation dependence and behaviour of passivation layers, J. Electrochem. Soc. 137 (1990) 3612–3626.

[2] I. Barycka, I. Zubel, Silicon anisotropic etching in KOH-isotropanol etchant, Sens. Actuators A 48 (1995) 229–238.
[3] E. Bassous, Fabrication of novel three-dimensional microstructures by the anisotropic etching of (1 0 0) and (1 1 0) silicon, IEEE Trans. Electron Devices ED25 (10) (1978) 1178–1185.
[4] K.E. Bean, Anisotropic etching of silicon, IEEE Trans. Electron Devices ED25 (10) (1978) 1185–1193.
[5] K.E. Peterson, Silicon as a mechanical material, Proc. IEEE 70 (1982) 420–457.
[6] S.-C. Chang, D.B. Hicks, The formation of microbridges on (1 0 0)-oriented silicon, J. Micromech. Microeng. 1 (1990) 25–29.
[7] W. Fang, Design of bulk micromachined suspensions, J. Micromech. Microeng. 8 (1998) 263–271.
[8] R.E. Oosterbroek, J.W. Berenschot, H.V. Jansen, A.J. Nijdam, G. Pandraud, A. Berg, M.C. Elwenspoek, Etching methodologies in ⟨1 1 1⟩-oriented silicon wafers, J. Microelectromech. Syst. 9 (3) (2000) 390–398.
[9] S. Lee, S. Park, D. Cho, The surface/bulk micromachining (SBM) process: a new method for fabricating released MEMS in single crystal silicon, J. Microelectromech. Syst. 8 (4) (1999) 409–416.
[10] G. Ensell, Free standing single-crystal silicon microstructures, J. Micromech. Microeng. 5 (1995) 1–4.
[11] W. Fang, J.A. Wickert, Determining mean and gradient residual stresses in thin films using micromachined cantilevers, J. Micromech. Microeng. 6 (1996) 301–309.
[12] L. Kiesewetter, J.M. Zhang, D. Houdeau, A. Steckenborn, Determination of Young's moduli of micromechanical thin films using the resonance method, Sens. Actuators A 35 (1992) 153–159.
[13] W. Fang, H.-C. Tsai, C.-Y. Lo, Determining thermal expansion coefficients of thin films using micromachined cantilevers, Sens. Actuators A 77 (1999) 21–27.
[14] W. Fang, J.A. Wickert, Post-buckling of micromachined beams, J. Micromech. Microeng. 8 (1994) 116–122.
[15] H. Guckel, T. Randazzo, D.W. Burns, A simple technique for the determination of mechanical strain in thin films with application to polysilicon, J. Appl. Phys. 57 (1985) 1671–1675.
[16] G.T.A. Kovacs, N.I. Maluf, K.E. Petersen, Bulk micromachining of silicon, Proc. IEEE 868 (1998) 1536–1551.
[17] C. Shafai, M.T. Brett, T.M. Hrudey, Etch-induced stress failure of SiO_2 cantilever beams, Sens. Actuators A 70 (1998) 283–290.
[18] J. Schweitz, A new and simple micromechanical approach to the stress-strain characterization of thin coatings, J. Micromech. Microeng. 1 (1991) 10–15.